

# Biomedical Microdevices

## Ethosomes and organogels for cutaneous administration of crocin

--Manuscript Draft--

<b>Manuscript Number:</b>	
<b>Full Title:</b>	Ethosomes and organogels for cutaneous administration of crocin
<b>Article Type:</b>	Manuscript
<b>Keywords:</b>	phospholipid, nanotechnology, viscosity, chemical stability, permeation enhancers
<b>Corresponding Author:</b>	Rita Cortesi Universita degli Studi di Ferrara Dipartimento di Scienze della Vita e Biotecnologie Ferrara, ITALY
<b>Corresponding Author Secondary Information:</b>	
<b>Corresponding Author's Institution:</b>	Universita degli Studi di Ferrara Dipartimento di Scienze della Vita e Biotecnologie
<b>Corresponding Author's Secondary Institution:</b>	
<b>First Author:</b>	Elisabetta Esposito
<b>First Author Secondary Information:</b>	
<b>Order of Authors:</b>	Elisabetta Esposito Markus Drechsler Nicolas Huang Gabriella Pavoni Rita Cortesi Debora Santonocito Carmelo Puglia
<b>Order of Authors Secondary Information:</b>	
<b>Funding Information:</b>	
<b>Suggested Reviewers:</b>	Sergey Shityakov DR., M.D., PhD, Universitatsklinikum Wurzburg Shityakov_S@ukw.de Lucas Toledo Dr. PhD, Universidade Estadual de Maringa lucastld@gmail.com Marieta Fundueanu-Constantin DR., M.D., PhD, Institutul de Chimie Macromoleculara Petru Poni constantinmarieta@yahoo.com

[Click here to view linked References](#)

# 1 **Ethosomes and organogels for cutaneous administration of crocin**

1  
2  
3  
4  
5  
6  
7  
8  
9  
10

3 Elisabetta Esposito<sup>a\*</sup>, Markus Drechsler<sup>b</sup>, Nicolas Huang<sup>c</sup>, Gabriella Pavoni<sup>a</sup>, Rita  
4 Cortesi<sup>a\*</sup>, Debora Santonocito<sup>d</sup> and Carmelo Puglia<sup>d</sup>

11  
12 <sup>6</sup> *<sup>a</sup>Department of Life Sciences and Biotechnologies, University of Ferrara, I-44121 Ferrara,*  
13  
14 <sup>7</sup> *Italy*

15  
16  
17 <sup>8</sup>  
18  
19 <sup>9</sup> *<sup>b</sup>Macromolecular Chemistry II, University of Bayreuth, Germany*

20  
21  
22 <sup>10</sup>  
23  
24 <sup>11</sup> *<sup>c</sup>Institut Galien Paris-Sud (CNRS UMR 8612), Faculté de Pharmacie, Université Paris-*  
25  
26 <sup>12</sup> *Sud, France*

27  
28  
29 <sup>13</sup>  
30  
31 <sup>14</sup> *<sup>d</sup>Department of Drug Science, University of Catania, I-95125-Catania, Italy*

32  
33  
34 <sup>15</sup>  
35  
36 <sup>16</sup> \*Correspondence to: Dr Elisabetta Esposito and Prof Rita Cortesi  
37  
38  
39 <sup>17</sup> Dipartimento SVEB  
40  
41 <sup>18</sup> Via Fossato di Mortara, 19  
42  
43  
44 <sup>19</sup> I-44121 Ferrara, Italy  
45  
46 <sup>20</sup> Tel. +39/0532/455259  
47  
48  
49 <sup>21</sup> Fax. +39/0532/455953  
50  
51 <sup>22</sup> e-mail [ese@unife.it](mailto:ese@unife.it); [crt@unife.it](mailto:crt@unife.it)

52  
53  
54  
55  
56  
57  
58  
59  
60  
61  
62  
63  
64  
65

24 **Abstract**

1  
25 The present study describes the production and characterization of phosphatidylcholine  
3  
4  
26 based ethosomes and organogels, as percutaneous delivery systems for crocin.

6  
27 Crocin presence did not influence ethosome morphology, while the drug slightly increased  
8  
9  
28 ethosome mean diameter. Importantly, the poor chemical stability of crocin has been found  
10  
11  
12  
29 to be long controlled by organogel. To investigate the performance of phosphatidylcholine  
13  
14  
30 lipid formulations as crocin delivery system, *in vivo* studies, based on tape stripping and  
15  
16  
31 skin reflectance spectrophotometry, were performed. Tape stripping results suggested a  
17  
18  
32 rapid initial penetration of crocin exerted by the organogel, probably due to a strong  
19  
20  
21  
33 interaction between the peculiar supramolecular aggregation structure of phospholipids in  
22  
23  
34 the vehicle and the lipids present in the stratum corneum and a higher maintenance of  
24  
25  
35 crocin concentration in the case of ethosomes, possibly because of the formation of a  
26  
27  
36 crocin depot in the stratum corneum. Skin reflectance spectrophotometry data indicated  
28  
29  
30  
31 that both vehicles promoted the penetration of crocin through the skin, with a more rapid  
32  
33  
34 anti-inflammatory effect exploited by ethosomes, attributed to an ethanol pronounced  
35  
36  
37 penetration enhancer effect and to the carrier system as a whole.

38  
39  
40  
41 **Keywords:** phospholipid, nanotechnology, viscosity, chemical stability, permeation  
42  
43  
44 enhancers

45  
46  
47  
48  
49  
50  
51 **Abbreviations:** Ethosomes (ETHO); organogels (ORG); crocin (CRO); xanthan gum (X  
52  
53  
54 GUM), phosphatidylcholine (PC); minimal erythematol dose (MED).

48 **1. Introduction**

1  
2  
3  
4  
5  
6  
7  
8  
9  
10  
11  
12  
13  
14  
15  
16  
17  
18  
19  
20  
21  
22  
23  
24  
25  
26  
27  
28  
29  
30  
31  
32  
33  
34  
35  
36  
37  
38  
39  
40  
41  
42  
43  
44  
45  
46  
47  
48  
49  
50  
51  
52  
53  
54  
55  
56  
57  
58  
59  
60  
61  
62  
63  
64  
65

Bioactive natural components, such as phytochemicals derived from edible plants, are effective in preventing or suppressing the process of carcinogenesis and other chronic diseases (Weng and Yen, 2012). For instance polyphenols, flavonoids, isoflavonoids, proanthocyanidins, phytoalexins, anthocyanidins and carotenoids have been recognized as potential skin cancer chemopreventive agents (Mittal et al, 2003; Suhr, 2003; Nanadakumar et al, 2008; Meeran et al, 2009; Weng and Yen, 2012;). Moreover many of them are under clinical study, being able to interfere with specific stages of the carcinogenic process (Wanga et al, 2012). Skin carcinogenesis is a multistep process which consists in malignant growth of the epidermis induced by chemical carcinogens or UV irradiation, generating reactive oxygen species (Robertson, 2012). In this respect cellular antioxidant and cytoprotective proteins can protect against skin carcinogenesis (Chun et al, 2014).

Crocin (CRO), the diester of the disaccharide gentiobiose and the dicarboxylic acid crocetin, is a carotenoid compound responsible for the colour of saffron, occurring naturally in crocus and gardenia fruit (Winterhalter and Straunbirger, 2000). Due to its powerful antioxidant properties, CRO could be useful in a number of pathologies, i.e. neurodegenerative disorders, atherosclerosis, depression and liver diseases (Alavizadeh and Hosseinzadeh, 2014). In addition CRO exerts significant antinociceptive and anti-inflammatory activity, as well as chemopreventive and anti-cancer properties, as suggested by different studies (Escribano et al, 1996; Konoshima et al, 1998).

Unfortunately, CRO is scarcely stable, indeed it loses most of its functionality after exposure to heat, oxygen, light and acids (Tsimidou and Tsatsaroni, 1993). Moreover it has been demonstrated that CRO has poor absorption and low bioavailability after oral

72 administration, being hydrolyzed by  $\beta$ -glucosidase and rapidly eliminated (Asai et al,  
1  
73 2005). Thus, despite its beneficial effects, CRO chemical instability and high susceptibility  
3  
44 to process conditions represent obstacles for its therapeutic application.  
5  
6  
7

85 In the present study, in an attempt to design topical vehicles for CRO able to improve its  
9  
10 stability, different phosphatidylcholine based nano-systems, such as ethosomes (ETHO)  
1176  
12 and organogels (ORG), have been considered.  
1377  
14  
15

16  
178 Phosphatidylcholine (PC), a versatile natural and biocompatible surfactant, is able to form  
18  
199 a number of supra-molecular structures (i.e. direct and inverted micelles or hexagonal,  
20  
21 cubic and lamellar phases), providing the opportunity to produce innovative (trans)dermal  
2280  
23 forms (Grdadolnik, 1991). Indeed due to its affinity with skin lipids, PC can exert  
2481  
25 penetration enhancer properties, increasing skin permeation (Wohlrab et al, 2010; Tian et  
2682  
27 al, 2012).  
28  
283  
30  
31

32  
3384 ETHO can be defined as lipid vesicular systems constituted of phospholipids (such as soy  
34  
35 PC), ethanol and water. ETHO find interesting application as percutaneous delivery  
36  
37 systems. Indeed the presence of ethanol in high concentrations (20-45%) confers to ETHO  
3886  
39 a soft structure which promotes enhancer delivery to/through the skin (Toitou et al, 2000).  
4087  
41  
4288 The penetration enhancement mechanisms of ETHO should be ascribed to fusion with  
43  
44 skin lipids, as well as to penetration of intact ETHO, as a function of ETHO composition  
4589  
46 and physical characteristics (Godin and Toitou, 2003; Jain et al, 2007).  
4790  
48  
49  
50

51 ORG are gel-like reverse micellar systems in which PC is solubilized in a biocompatible oil  
52  
53 (Rault et al, 2012). Particularly, the addition of a precise amount of water to a PC oil  
5492  
55 solution initially leads to production of spherical reversed micelles, afterwards the micellar  
5693  
57 aggregates intertwine, forming a three-dimensional network in the bulk phase. Their  
5894  
59 peculiar structure and the possibility to modulate the system viscosity make ORG suitable  
6095  
61  
62  
63  
64  
65

96 for (trans)cutaneous administration of hydrophilic and lipophilic molecules (Patil et al,  
1  
2  
3 97 2011; Esposito et al, 2013).  
4  
5

6  
7 98 In the present investigation, the efficiency of ETHO and ORG as cutaneous delivery  
8  
9 99 systems for CRO has been studied.  
10

11  
12 100 Notably, the capability of ETHO and ORG to control CRO stability has been investigated.  
13

14 101 Special regard has been devoted to an *in vivo* investigation aimed to study CRO amount in  
15  
16 102 *stratum corneum* and CRO anti-inflammatory activity after cutaneous application.  
17  
18

19 103  
20  
21  
22  
23  
24  
25  
26  
27  
28  
29  
30  
31  
32  
33  
34  
35  
36  
37  
38  
39  
40  
41  
42  
43  
44  
45  
46  
47  
48  
49  
50  
51  
52  
53  
54  
55  
56  
57  
58  
59  
60  
61  
62  
63  
64  
65

104 **2. Materials and methods**

1  
105  
3

106 **2.1. Materials**

6  
107  
8

108 Crocin (CRO, crocetin digentibiose ester), xanthan gum (X GUM) and isopropylpalmitate  
109 were purchased from Sigma Chemical Company (St Louis, MO, USA). The soybean  
110 lecithin (PC) (90% phosphatidylcholine) used for ETHO and ORG preparation was  
111 Epikuron 200 from Lucas Meyer, Hamburg, Germany. Solvents were of HPLC grade and  
112 all other chemicals were of analytical grade.

21  
113  
22

114 **2.2. Production of ethosomes**

25  
115  
26

116 For the preparation of ETHO, PC (30 mg/ml) was first dissolved in ethanol (30%, v/v).  
117 Afterwards isotonic Palitzsch buffer (IPB) (5 mM Na<sub>2</sub>B<sub>4</sub>O<sub>7</sub>, 180 mM H<sub>3</sub>BO<sub>3</sub>, 18 mM NaCl),  
118 was slowly added to the ethanolic solution under continuous stirring at 700 rpm by an IKA  
119 Eurostar digital (IKA Labortechnik Janke & Kunkel, Staufen, Germany). Mechanical stirring  
120 was performed for 30 min at room temperature in the dark. In the case of CRO containing  
121 ETHO (ETHO-CRO), CRO (0.5 mg/ml) was added to IPB before addition to PC ethanol  
122 solution. Table 1 reports the ETHO composition.

123 In order to obtain homogeneously sized vesicles, ETHO-CRO were subjected to two  
124 extrusion cycles through 400 nm pore size polycarbonate filters.

50  
125  
52

126 **2.3. Characterization of ethosomes**

54  
127  
55

128 *2.3.1 Cryo-Transmission Electron Microscopy (Cryo-TEM)*

59  
129  
60

130 Samples were vitrified as described in a previous study (Esposito et al, 2012). Briefly a  
1 sample droplet of 2 uL was put on a lacey carbon filmed copper grid (Science Services,  
131 Muenchen) for 30 s. Subsequently, most of the liquid was removed with blotting paper  
132 leaving a thin film stretched over the lace holes. The specimens were instantly shock  
133 frozen by rapid immersion into liquid ethane cooled to approximately 90 K by liquid  
134 nitrogen in a temperature-controlled freezing unit (Zeiss Cryobox, Carl Zeiss Microscopy  
135 GmbH, Jena, Germany). The temperature was monitored and kept constant in the  
136 chamber during all the sample preparation steps. After freezing the specimens, the  
137 remaining ethane was removed using blotting paper. The vitrified specimen was  
138 transferred to a Zeiss/Leo EM922 Omega EFTEM (Zeiss Microscopy GmbH, Jena,  
139 Germany) transmission electron microscope using a cryoholder (CT3500, Gatan, Munich,  
140 Germany). Sample temperature was kept below 100K throughout the examination.  
141 Specimens were examined with reduced doses of about 1000-2000 e/nm<sup>2</sup> at 200 kV.  
142 Images were recorded by a CCD digital camera (Ultrascan 1000, Gatan, Munich,  
143 Germany) and analysed using a GMS 1.9 software (Gatan, Munich, Germany).

### 146 *2.3.2 Photon Correlation Spectroscopy (PCS)*

147 Submicron particle size analysis was performed using a Zetasizer 3000 PCS (Malvern  
148 Instr., Malvern, England) equipped with a 5 mW helium neon laser with a wavelength  
149 output of 633 nm. Glassware was cleaned of dust by washing with detergent and rinsing  
150 twice with sterile water. Measurements were made at 25 °C at an angle of 90° with a run  
151 time of at least 180 s. Samples were diluted with bidistilled water in a 1:10 v:v ratio. Data  
152 were analysed using the "CONTIN" method (Pecora, 2000). Measurements were  
153 performed in triplicate on freshly prepared samples and after 6 months from production.

## 155 **2.4. CRO content of ethosomes**



156  
1  
157  
3  
158  
4  
5  
6  
159  
7  
8  
160  
9  
10  
161  
11  
162  
12  
13  
163  
14  
15  
16  
164  
17  
18  
19  
20  
21  
22  
23  
24  
25  
26  
27  
28  
29  
30  
31  
32  
33  
34  
35  
36  
37  
38  
39  
40  
41  
42  
43  
44  
45  
46  
47  
48  
49  
50  
51  
52  
53  
54  
55  
56  
57  
58  
59  
60  
61  
62  
63  
64  
65

The entrapment capacity (EC) of CRO in ETHO was determined (Toitou et al., 2000). 100 µl aliquot of ETHO-CRO was loaded in a centrifugal filter (Microcon centrifugal filter unit YM-10 membrane, NMWCO 10 kDa, Sigma Aldrich, St Louis, MO, USA) and centrifuged (Spectrafuge™ 24D Digital Microcentrifuge, Woodbridge NJ, USA) at 8,000 rpm for 20 min. The amount of free and entrapped CRO was determined by dissolving the supernatant with a known amount of ethanol (1:10, v/v). The amount of CRO in the supernatant was determined by high performance liquid chromatography (HPLC) method, as below reported. The EC was determined as follows:

$$(1) \quad EC = \frac{T_{CRO} - S_{CRO}}{T_{CRO}} \times 100$$

where  $T_{CRO}$  stands for the total amount of CRO added to the formulation and  $S_{CRO}$  for the amount of drug measured in the supernatant.

## 2.5. Production of organogels

Production of ORG was conducted by adding precise amounts of water to PC (200 mM) solution in isopropylpalmitate, under stirring. The amount of added water has been expressed as the molar water to PC ratio ( $[water]/[PC]$ ) (Schipunov, 2001).  $[Water]/[PC]_{max}$  was determined, i.e. the highest amount of water that can be incorporated into the PC solution with no phase separation. The samples were maintained under stirring at 25° C for 30 minutes and later examined under a Leitz diaplan microscope (Lietz Wetzlar, Germany) equipped with a polarizer positioned in the light pass before the specimen.

180 To produce CRO containing ORG (ORG-CRO), CRO was previously solubilized in water  
181 before addition to PC solution. CRO final concentration in ORG-CRO was 0.05 % w/v.  
182 Table 1 reports the ORG composition.

## 184 2.6. Prediction of long-term stability

186 The stability of CRO was assessed in aqueous solution, ETHO-CRO and ORG-CRO  
187 stored in glass containers at 25°C for 3 months.

188 Chemical stability was evaluated, determining CRO content by HPLC analyses. Shelf life  
189 values were calculated as below reported (Pugh, 2007).

190 Log (CRO residual content, %) was plotted against time and the slopes (m) were  
191 calculated by linear regression.

192 The slopes (m) were then substituted into the following equation for the determination of k  
193 values:

$$195 \quad (2) \quad k = m \times 2.303$$

197 Shelf life values (the time for 10% loss,  $t_{90}$ ) and half-life (the time for 50% loss,  $t_{1/2}$ ) were  
198 then calculated by the following equations:

$$200 \quad (3) \quad t_{90} = 0.105/k$$

$$202 \quad (4) \quad t_{1/2} = 0.693/k$$

## 204 2.7. Gel production

206 Ethosome viscosity has been improved by adding x-gum (1% w/w) directly into the  
1  
207 dispersion and by slowly stirring for 1 hour until complete dispersion of the gum. The  
3  
208 obtained viscous ETHO formulation has been named ETHO-CRO X-GUM.  
4  
6

209

## 210 **2.8. Rheological measurements**

211

212 Rheological measurements were performed with an AR-G2 rotational rheometer (TA  
15  
213 Instruments). The geometry used was an aluminium cone-plate with a diameter of 40 mm  
18  
214 and an angle of 1°. Flow curves were obtained by increasing the shear rate from 0.01 s<sup>-1</sup>  
20  
215 to 5000 s<sup>-1</sup> with 5 points per decade, each point was maintained for a duration of 180 s in  
23  
216 order to perform measurements in the permanent regime. The temperature was set at  
25  
217 25°C or 35°C and controlled with a Peltier plate. A solvent trap was used to prevent water  
28  
218 evaporation. Measurements were performed in triplicate for each sample, to ensure  
30  
219 reproducibility.  
32

220

## 221 **2.9. In vivo studies**

222

### 223 *2.9.1 Volunteers recruitment*

224

225 *In vivo* experiments were performed on two groups of ten volunteers: group A enrolled for  
47  
226 the first *in vivo* experimentation (tape-stripping) and group B enrolled for the second one  
49  
227 (evaluation of anti-inflammatory activity).  
52

228 Experiments were conducted in accordance with The Code of Ethics of the World Medical  
54  
229 Association (Helsinki Declaration 1964) and its later amendments for experiments  
57  
230 involving humans.  
59

60

61

62

63

64

65

231 The volunteers were of both sexes in the age range 25–55 years and recruited after  
1  
232 medical screening including the filling of a health questionnaire followed by physical  
3  
233 examination of the application sites. Informed consent was obtained from all individual  
4  
6  
234 participants included in the study. The participants did not suffer from any ailment and  
8  
235 were not on any medication at the time of the study. They were rested for 15 min prior to  
10  
11  
236 the experiments and room conditions were set at 22±2 °C and 40–50% relative humidity.  
13

### 237 15 16 238 2.9.2 Tape Stripping

18  
239  
20  
21  
240 For each subject (group A), ten sites on the ventral surface of each forearm were defined  
23  
241 using a circular template (1 cm<sup>2</sup>) and demarcated with permanent ink. One of the ten sites  
25  
242 of each forearm was used as control, three sites were treated with 300 mg of ETHO-CRO-  
27  
28  
243 X GUM, three sites were treated with 300 mg of ORG-CRO and the remaining three with  
30  
31  
244 300 mg of X GUM-CRO. The preparations were spread uniformly by means of a solid  
32  
33  
245 glass rod and then the sites were occluded for 6 h using Hill Top Chambers (Hill Top  
35  
36  
246 Research, Cincinnati, OH). After the occlusion period, the residual formulations were  
37  
38  
247 removed by gently wiping with cotton balls (different for each pretreated site). Ten  
40  
248 individual 2 cm<sup>2</sup> squares of adhesive tape (Scotch Book Tape 845, 3M) were utilized to  
42  
43  
249 sequentially tape-strip the *stratum corneum* on the application sites. The removal of  
45  
250 *stratum corneum* in each pretreated site was effected at 1 h (t = 1), 3 h (t = 3) and 6 h (t =  
47  
48  
251 6) after formulation removal (Esposito et al., 2014).

50  
252 Each adhesive square, before and after skin tape stripping, was weighed on a semi-micro  
52  
53  
253 balance (sensitivity 1mg, Sartorius model ME415S, Goettingen, Germany) to quantify the  
54  
55  
254 weight of removed *stratum corneum*. After each stripping, the tapes were put in the same  
57  
255 vial containing 2 ml of the HPLC mobile phase methanol:water (65:35 v/v) and subjected  
59  
60  
256 to vortical stirring over 30 s. The extracted CRO was then quantified by HPLC. The  
62  
63  
64  
65

257 recovery of CRO was validated by spiking tape-stripped samples of untreated *stratum*  
1  
258 *corneum* with 2 ml of a mobile phase containing CRO 10 mg/ml. The extraction efficiency  
3  
259 of CRO was  $97.2 \pm 0.5 \%$  (n= 3).  
4  
6

260

### 261 2.9.3 *In vivo anti-inflammatory activity*

262

263 The *in vivo* anti-inflammatory activity has been evaluated by measuring the inhibition of the  
15  
264 UVB-induced skin erythema. In particular, the UVB-induced skin erythema was monitored  
16  
18  
265 by using a reflectance visible spectrophotometer X-Rite model 968 (XRite Inc. Grandville,  
20  
266 MI, USA), calibrated and controlled as previously reported (Esposito et al, 2005).  
21  
23  
267 Reflectance spectra were obtained over the wavelength range 400–700 nm using  
25  
268 illuminant C and 2° standard observer. From the spectral data obtained, the erythema  
26  
27  
28  
269 index (EI) was calculated using Eq. (5).  
30

270

$$(5) \quad E.I. = 100 \left[ \log \frac{1}{R_{560}} + 1.5 \left( \log \frac{1}{R_{540}} + \log \frac{1}{R_{580}} \right) - 2 \left( \log \frac{1}{R_{510}} + \log \frac{1}{R_{610}} \right) \right]$$

272

273 where 1/R is the inverse reflectance at a specific wavelength (560, 540, 580, 510 and  
38  
40  
274 610). The skin erythema was induced by UVB irradiation using a UVM-57 ultraviolet lamp  
42  
275 (UVP, San Gabriel, CA, USA) ultraviolet lamp emitting in 290–320 nm range, with 302 nm  
43  
45  
276 output peak, the rate measured at the skin surface was 0.80 mW/cm<sup>2</sup>. The minimal  
47  
277 erythematol dose (MED) was preliminarily determined, and an irradiation dose  
48  
49  
50  
278 corresponding to twice the value of MED was used throughout the study. For each subject  
52  
279 (group B), seven sites on the ventral surface of each forearm were defined using a circular  
53  
54  
280 template (1 cm<sup>2</sup>) and demarcated with permanent ink. One of the seven sites of each  
55  
57  
281 forearm was used as control, three sites were treated with 300 mg of ETHO-CRO-X GUM  
58  
59  
282 and the remaining three with 300 mg of ORG-CRO. The preparations were spread  
60  
61  
62  
63  
64  
65

283 uniformly by means of a solid glass rod and then the sites were occluded for 6 h using Hill  
1  
284 Top Chambers (Hill Top Research, Cincinnati, OH). After the occlusion period, the  
3  
285 chambers were removed and the skin surfaces were gently washed and allowed to dry for  
4  
5  
6  
286 15 min. Each pre-treated site was exposed to UV-B irradiation 1, 3 and 6 h (t = 1, t = 3 and  
8  
287 t = 6, respectively) after ETHO-CRO-X GUM and ORG-CRO removal and the induced  
10  
288 erythema was monitored for 52 h. EI baseline values were taken at each designated site  
11  
12  
13  
289 before application of gel formulation and they were subtracted from the EI values obtained  
15  
16  
290 after UV-B irradiation at each time point to obtain  $\Delta$ EI values. For each site, the AUC was  
18  
19  
20  
291 computed using the trapezoidal rule. To better outline the results obtained, the PIE  
21  
292 (percentage of inhibition of erythema) was calculated from the AUC values using Eq. (6):  
23

293  
24  
25  
26  
294 (6) 
$$\text{Inhibition (\%)} = \frac{\text{AUC}_{(C)} - \text{AUC}_{(T)}}{\text{AUC}_{(C)}} \times 100$$
  
28  
295  
30

31  
296 where  $\text{AUC}_{(C)}$  is the area under the response/time curve of the vehicle-treated site  
33  
297 (control) and  $\text{AUC}_{(T)}$  is the area under the response/time curve of the drug-treated site.  
35  
36  
37

#### 38 299 2.9.4 Statistical Analysis 40

39  
300  
41  
42  
43  
301 Statistical differences of *in vivo* data were determined using repeated-measures analysis  
45  
302 of variance (ANOVA) followed by the Bonferroni-Dunn post hoc pairwise comparison  
47  
48  
303 procedure. The employed software was Prism 5.0, Graph Pad Software Inc. (La Jolla, CA -  
50  
304 USA). A probability of less than 0.05 is considered significant in this study.  
52  
53

#### 54 305 55 306 2.10 HPLC Procedure 57

58  
59

308 HPLC determinations were performed using a quaternary pump (Agilent Technologies  
1  
309 1200 series, USA) an UV-detector operating at 440 nm, and a 7125 Rheodyne injection  
3  
310 valve with a 50 µl loop. Samples were loaded on a stainless steel C-18 reverse-phase  
4  
6  
311 column (15×0.46 cm) packed with 5 µm particles (Grace® - Alltima, Alltech, USA).  
8  
312 Elution was performed with a mobile phase containing methanol:water (65:35, v/v); at a  
9  
10  
313 flow rate of 0.8 ml/min, retention time was 4.5 min. The method was validated for linearity  
11  
13  
314 (R<sub>2</sub> = 0.995), repeatability (relative standard deviation 0.01%, n=6 injections) and limit of  
14  
15  
315 quantification (0.04 µg/ml).  
16  
18

316  
20

21  
22  
23  
24  
25  
26  
27  
28  
29  
30  
31  
32  
33  
34  
35  
36  
37  
38  
39  
40  
41  
42  
43  
44  
45  
46  
47  
48  
49  
50  
51  
52  
53  
54  
55  
56  
57  
58  
59  
60  
61  
62  
63  
64  
65

### 317 **3. Results**

1  
318

#### 319 **3.1. Preparation and characterization of ethosomes**

6  
320

321 Production of ETHO was spontaneously obtained by slow addition of an aqueous buffer to  
10  
322 a PC ethanol solution under continuous stirring at room temperature. The presence of  
13  
323 ethanol allowed to solubilize PC and to confer initial optical transparency to the dispersion.  
15  
324 The addition of IPB buffer resulted in an increase of turbidity, suggesting the formation of  
18  
325 ethosomal vesicles. In the case of CRO containing ETHO, the presence of the drug  
20  
326 conferred a yellow colour to the dispersion (as shown in Online Resource 1 A).

23  
327 The morphological analysis of ETHO investigated by cryo-TEM, shown in Fig. 1, revealed  
25  
328 the presence of multilamellar spherical vesicles and multivesicular vesicles, both in the  
27  
329 case of ETHO (Fig. 1 A, B) and ETHO-CRO (Fig. 1 C, D). At the highest magnification the  
30  
330 presence of a double layer in ETHO vesicle conformation can be observed (Fig. 1 B, D).

33  
331 Table 2 summarizes the dimensional distribution of ETHO dispersions obtained by PCS  
35  
332 analysis. Vesicle mean diameter was 332 and 454 nm in the case of ETHO and ETHO-  
37  
333 CRO, respectively. Particularly vesicles were characterized by a bimodal dimensional  
40  
334 distribution (PI 0.32 and 0.38). The presence of CRO slightly increased both mean  
42  
335 diameter and polydispersity of vesicles. In order to obtain homogeneous monolamellar  
45  
336 vesicles, ETHO-CRO vesicles have been extruded through polycarbonate membranes  
47  
337 with calibrated pores (400 and 200 nm), this strategy led to a decrease of mean diameter  
49  
338 up to 250 nm, PI 0.28.

50  
339 After 6 months from production, mean diameters underwent a 48 or 18% increase in the  
54  
340 case of ETHO and ETHO-CRO respectively.

57  
341

59  
342

#### 342 **3.2. Preparation of organogels**

62  
63  
64  
65



343 Production of ORG was conducted by adding precise amounts of water to reverse micellar  
1  
344 solutions constituted of PC solubilized in isopropylpalmitate. After 30 min of magnetic  
3  
345 stirring, transparent gels were obtained, whose consistency was a function of the amount  
4  
6  
346 of added water (as shown in Online Resource 1 B). Particularly 1:1, 2:1 and 3:1  
8  
9  
347 [water]/[PC] ratio have been considered (Online Resource 1 B). (Luisi et al, 1990). Since  
10  
11  
348 the [water]/[PC]<sub>max</sub> was found to be 3:1, the corresponding amount of water was selected  
13  
14  
349 for ORG and ORG-CRO production. Both ORG and ORG-CRO were transparent, yellow,  
15  
16  
350 macroscopically monophasic and isotropic under polarized light.  
18

351  
20  
21

### 352 3.3. Entrapment capacity (EC)

23

24  
253

26  
354 The preparation of ETHO-CRO and ORG-CRO was spontaneously performed at 25°C  
28  
355 under magnetic stirring in dark vials, preventing drug loss on mechanical devices, as well  
30  
31  
356 as thermal or light degradation. For this reason, it was reasonable to obtain almost  
33  
34  
357 quantitative recovery of drug into the formulations.  
35

36  
358 Nonetheless it should be considered that in the case of ORG-CRO, being constituted of  
38  
39  
359 reverse micelles, CRO was entrapped inside the micelles in the aqueous environment,  
40  
41  
360 while in the case of ETHO-CRO, CRO was expected to be dissolved partly inside the  
43  
361 vesicles and partly within the aqueous environment out of the vesicles (Fig. 2). Therefore,  
45  
362 the ultracentrifugation method was employed in order to calculate the EC (Toitou et al,  
47  
48  
363 2000).  
50

51  
364 The obtained data indicate that CRO inside the vesicles was 74%, while the amount of  
52  
53  
365 CRO out of the vesicle was 26% (Table 3).  
55

56  
366 It should be underlined that the strategy of extruding ETHO-CRO resulted in a loss of the  
57  
58  
367 drug. Indeed the extrusion process led to an escape of CRO, finally resulting in a 48±3%  
60  
61  
62  
63  
64  
65

368 EC value for ETHO-CRO. For this reason ETHO-CRO have been employed for in vivo  
1  
369 studies as they were.  
3

370 For in vivo experiments CRO amount in ETHO-CRO and in ORG-CRO was the same,  
4  
6  
371 because untrapped CRO was not separated from ETHO-CRO vesicles.  
8

372  
10

### 373 **3.4. Crocin stability**

11  
13

374  
15

375 CRO content in ETHO-CRO and ORG-CRO was determined as a function of time and  
16  
18  
376 expressed as percentage of the total amount used for the preparation (Fig. 3). It is evident  
20  
21  
377 that the degradation of CRO was more controlled by ORG-CRO than by ETHO-CRO,  
23  
378 indeed CRO residual content after 3 months was 78% and 30%, respectively. Conversely  
25  
379 CRO solution was almost completely degraded after 15 days.  
27

380 Table 3 reports shelf life ( $t_{90}$ ) and half life ( $t_{1/2}$ ) values calculated by equations (3) and (4).  
28  
30

381 It was found that ORG could maintain 90% of CRO stability for almost 38 days, whilst in  
31  
32  
33  
382 the case of ETHO,  $t_{90}$  was 7 days. The  $t_{1/2}$  values reached almost 8 months in the case of  
35  
383 ORG-CRO, and 2 months in the case of ETHO-CRO. All data were statistically significant  
37  
38  
384 ( $p < 0.0001$ ).  
40

385 Nevertheless both ETHO-CRO and ORG-CRO did not show changes in physical  
42  
43  
386 appearance by time, maintaining homogeneous aspect, absence of phase separation  
45  
387 phenomena and/or aggregates also after six months from production.  
47

388  
49

### 389 **3.5. Gelation of ethosomes and rheological analyses**

50  
52

390  
53

391  
55

391 ORG-CRO with 3:1 [water]/[PC] ratio is characterized by a suitable viscosity for cutaneous  
56  
58  
392 administration ( $8.03 \pm 0.3$  Pa.s at  $25^\circ\text{C}$ , shear rate  $10 \text{ s}^{-1}$ ). Instead, the low viscosity of  
60

393  
61

394  
62

395  
63

396  
64  
65

393 ETHO-CRO, did not enable its topical application, for this reason X GUM was directly  
1  
394 added into ETHO dispersion. The resulting ETHO-CRO-X GUM possessed a viscosity  
3  
395 adequate for cutaneous administration, being  $2.72 \pm 0.2$  Pa.s at  $25^\circ\text{C}$ , shear rate  $10 \text{ s}^{-1}$ .  
4  
5  
6

396 Fig. 4 shows flow curves for ETHO-CRO-X GUM (A), ORG-CRO (B) and CRO-X GUM  
8  
397 (C). In particular the viscosity vs. shear rate has been measured at  $25^\circ\text{C}$  (grey profile) and  
10  
398  $35^\circ\text{C}$  (black profile), in order to mimic storage condition or skin application, respectively.  
11  
12  
13

399 The points on the curves are the means of three experiments and error bars represent  
15  
400 standard deviation. All samples were very slightly thixotropic, indeed the upward and down  
16  
17  
18  
401 curves are almost superimposed.  
19  
20

402 In Fig 4A and 4C, flow curves exhibit a marked non-Newtonian shear thinning behavior:  
21  
22  
23  
403 the steady shear viscosity sharply decreased as an increase in shear rate. In addition, the  
24  
25  
404 first and second Newtonian plateaux are not observed at low and high shear rates  
26  
27  
28  
405 respectively. The temperature did not influence the behaviour of the material, in fact the  
29  
30  
406 curves at  $25^\circ\text{C}$  or  $35^\circ\text{C}$  are superimposable.  
31  
32

407 In Figure 4B ORG-CRO shows an initial Newtonian plateau at both temperature followed  
33  
34  
35  
408 by a shear thinning behaviour: the Newtonian plateau extends from  $0.01 \text{ s}^{-1}$  to  $2 \text{ s}^{-1}$  (at 25  
36  
37  
38  
409  $^\circ\text{C}$ ) or  $10 \text{ s}^{-1}$  (at  $35^\circ\text{C}$ ), and the viscosity decreases significantly after the Newtonian  
39  
40  
410 plateaux. Indeed, the shear is then high enough to break significantly the structure of the  
41  
42  
411 gel (shear thinning behaviour) and, above  $200 \text{ s}^{-1}$ , to conceal the effect of temperature.  
43  
44  
45

412 Below  $200 \text{ s}^{-1}$ , the viscosity is higher at  $25^\circ\text{C}$  than at  $35^\circ\text{C}$ , with a difference of one order  
46  
47  
413 of magnitude at the Newtonian plateaux. The second Newtonian plateau can't be  
48  
49  
50  
414 observed, even at the maximum shear rate of the experiment: the microscopic structure of  
51  
52  
415 the material could be possibly modified at higher shear rate.  
53  
54

416 Flow curves of ETHO, ORG and X GUM are not shown since they are superimposable to  
55  
56  
57  
417 the reported curves. Indeed, the presence of CRO did not influence the viscosity of the  
58  
59  
418 material.  
60  
61  
62  
63  
64  
65

419  
1  
420  
3  
421  
4  
6  
422  
8  
423  
10  
424  
11  
13  
425  
14  
15  
426  
16  
18  
427  
20  
428  
21  
22  
23  
429  
25  
430  
26  
27  
28  
431  
30  
432  
31  
32  
33  
433  
35  
434  
37  
38  
435  
40  
436  
42  
437  
44  
45  
438  
47  
439  
48  
49  
50  
440  
52  
441  
54  
55  
442  
57  
443  
59  
444  
60  
61  
62  
63  
64  
65

### 3.6. Tape-stripping evaluation

The tape stripping experiment was employed for quantifying drug presence in the viable epidermis and the amount of CRO responsible for the anti-inflammatory effect (Esposito et al, 2005; Esposito et al, 2014). Formulations have been applied and removed from the forearms as depicted in the scheme of Fig. 5 A. From the analysis of the data reported in Fig. 5 B, both ETHO-CRO-X GUM and ORG-CRO induced a depletion in the amount of CRO in the stratum corneum. Notably in the case of ORG-CRO the depletion was more intense, indeed after 1, 3 and 6 h the amount of CRO was 1/2, 1/3 and 1/6 with respect to ETHO-CRO-X GUM. Contrarily, in the case of X GUM-CRO, CRO amount was nearly the same all over the period after formulation removal. Importantly the amounts of CRO recovered in the stratum corneum after removal of ETHO-CRO-X GUM, ORG-CRO and X GUM-CRO were significantly different.

### 3.7. In vivo anti-inflammatory activity

Since CRO can exert anti-inflammatory activity (Christodoulou et al, 2015; Nam et al, 2010), ETHO-CRO-X GUM and ORG-CRO were further investigated to determine their *in vivo* ability to inhibit the UVB-induced skin erythema. Skin reflectance spectrophotometry was used to determine the extent of the erythema and to assess the inhibition capacity of the formulations after their preventive application onto the skin. Fig. 6 A outlines the design of application of formulations on the forearm of volunteers. For each subject the AUC was determined plotting  $\Delta EI$  values versus time. The PIE values reported in Fig. 6 B indicate that after 1 h from the removal of formulations, ETHO-CRO-X GUM was more effective than ORG-CRO in inhibiting the induced erythema, while at 3 and 6 hours ORG-CRO

445 induced a higher inhibitory ability, respectively double and quadruple with respect to  
1  
446 ETHO-CRO-X GUM ( $p < 0.05$ ).

447

2  
3  
4  
5  
6  
7  
8  
9  
10  
11  
12  
13  
14  
15  
16  
17  
18  
19  
20  
21  
22  
23  
24  
25  
26  
27  
28  
29  
30  
31  
32  
33  
34  
35  
36  
37  
38  
39  
40  
41  
42  
43  
44  
45  
46  
47  
48  
49  
50  
51  
52  
53  
54  
55  
56  
57  
58  
59  
60  
61  
62  
63  
64  
65

#### 448 4. Discussion

1  
2  
3  
449 In this study, in order to find cutaneous vehicles able to control CRO instability, different  
4  
5  
450 PC based nanosystems have been explored. The entrapment of the drug in ETHO and  
7  
451 ORG has been spontaneously obtained upon addition of CRO solution to PC respectively  
9  
10  
452 solubilized in ethanol or in isopropylpalmitate. In both cases the production procedure did  
12  
453 not imply heating or high energy input, avoiding in this way physico-chemical stresses  
14  
15  
454 towards the labile CRO molecule (Tsimidou and Tsatsaroni, 1993).  
16  
17

18  
19  
455 The different supramolecular organization of PC resulted in the formation of spherical  
20  
21  
456 multilamellar vesicles in the case of ETHO-CRO or in an entanglement of extended worm-  
23  
457 like reverse micelles in the case of ORG-CRO. Thus the former is an aqueous low viscous  
25  
26  
458 dispersion, while the latter is a w/o microemulsion with a viscosity depending on the  
28  
459 amount of added water. As expected, in the case of ETHO-CRO, EC was not quantitative  
30  
31  
460 since the hydrophilic drug (log P -4.72) distributed partly in the aqueous environment  
32  
33  
461 outside the vesicles, contrarily ORG-CRO allowed complete entrapment of CRO in the  
35  
36  
462 aqueous domain inside the reverse micelles. ETHO-CRO have been employed for in vivo  
37  
38  
463 studies as they were, with no separation of the amount of CRO out of the vesicles and  
40  
41  
464 without extrusion. Indeed the extrusion process resulted not only in a decrease of vesicle  
42  
43  
465 mean diameter, but also in a halving of CRO entrapment in the vesicles due to CRO  
45  
466 leakage. Concerning ETHO-CRO mean diameter, it should be taken in consideration that  
47  
48  
467 the final gel formulations were designed for a cutaneous administration and not for a  
49  
50  
468 parenteral one, where mean diameter plays a fundamental role.  
52  
53

54  
55  
469 The peculiar CRO location has accounted for the different stabilizing power of ETHO-CRO  
56  
57  
470 and ORG-CRO, indeed in the case of ETHO-CRO the drug is partly distributed outside the  
58  
59  
471 vesicles and thus more exposed to chemical degradation, actually ORG-CRO was 5 fold  
60  
61  
62  
63  
64  
65

472 more efficacious than ETHO-CRO in controlling CRO degradation. However both  
1  
473 formulations remarkably controlled CRO stability with respect to plain solution, in fact it  
3  
474 should be underlined that CRO in water was rapidly decomposed ( $t_{1/2}$  2.26 days) (Table 3).  
4  
6  
7  
475 ORG-CRO was constituted of PC 200 mM, a concentration effective for penetration  
9  
10  
476 enhancement, isopropylpalmitate, a biocompatible oil particularly suitable for transdermal  
12  
477 delivery, and water (Fiume, 2001; Changez et al, 2006). In ORG-CRO the reverse micelles  
14  
478 initially formed, upon further addition of water linearly grew and entangled, finally  
16  
17  
479 constituting a three-dimensional network of interpenetrating worm-like micelles, stabilized  
19  
20  
480 by hydrogen bonds between PC and polar solvent molecules (Vintiloiu and Leroux, 2008;  
21  
22  
481 Kumar and Katare, 2005). While ORG-CRO possessed a viscosity suitable for cutaneous  
24  
482 application, ETHO-CRO required an improvement of viscosity by direct X GUM addition.  
26  
27  
28  
483 Rheology studies evidenced a steady shear flow behaviour typical of X GUM dispersions  
30  
31  
484 for ETHO-CRO-X GUM (Song et al, 2006). Indeed it can be suggested that X GUM  
32  
33  
485 molecules aggregate through hydrogen bonding and polymer entanglement, leading to a  
35  
486 high shear viscosity at low shear rates or at rest (Marcotte et al, 2001). The increase in  
37  
38  
487 shear rate caused a decrease of the steady shear viscosity since the polymer network  
40  
488 disentangled and to individual macromolecules align in the shear flow direction, resulting in  
42  
43  
489 a low shear viscosity at high shear rate region. Shear removal resulted in reconstitution of  
45  
490 network structure, rapidly recovering the viscosity (Vintiloiu and Leroux, 2008). ETHO  
47  
48  
491 presence did not influence the rheology behaviour of ETHO X-GUM.  
49  
50  
492 In the case of ORG-CRO the typical rheological behaviour of PC ORG was observed.  
52  
493 Indeed, as previously found, the vehicles exhibited a Newtonian flow over the low shear  
54  
55  
494 rate range, with a near constant viscosity, suggesting that the micelle network did not  
57  
495 break in this range (Schipunov and Hoffmann, 2000; Hashizaki et al, 2008).  
59  
60  
61  
62  
63  
64  
65

496 A further increment in shear rate led ORG-CRO to behave as a non-Newtonian fluid,  
1  
497 displaying a decrease in viscosity. This behaviour could be attributed to a breakage of the  
3  
498 micelle network structure provoked by the shear rate increment (Schipunov and Hoffmann,  
4  
5  
6  
499 2000; Hashizaki et al, 2008).  
8  
9

10  
500 CRO cutaneous biodistribution after application of ETHO-CRO-X GUM or ORG-CRO has  
11  
12  
501 been investigated by tape stripping and reflectance spectroscopy. The tape-stripping  
13  
14  
502 technique allows direct quantification of drug amounts in the *stratum corneum*, while  
15  
16  
17  
503 reflectance spectroscopy is able to give information about the concentration of CRO in the  
18  
19  
20  
504 viable epidermis since it measures the anti-inflammatory effect due to CRO presence in  
21  
22  
23  
505 the blood. In this respect the two methods can be considered complementary. In particular  
24  
25  
506 reflectance spectrophotometry monitors the degree of skin reddening. Before discussing  
26  
27  
507 the results, a brief methodological comment is in order. From reflectance spectra,  
28  
29  
30  
508 generally in the range of 400-700 nm, the values of different colour space systems  
31  
32  
509 (CIELab, Lch, etc.) can be obtained using different International Commission on  
33  
34  
35  
510 Illumination, CIE illuminants (C, D, A, etc.) and 2 or 10° illuminant observer. From spectral  
36  
37  
511 data it is possible to calculate at different wavelengths the relative reflectance or the  
38  
39  
512 logarithm of inverse reflectance (LIR), which is related to the light absorption of skin  
40  
41  
42  
513 chromophores (hemoglobin, melanin, etc.). The EI obtained from skin reflectance spectral  
43  
44  
514 values is thought to give a more accurate and reliable evaluation of skin erythema  
45  
46  
47  
515 (Harrison et al, 2004). Since this is due to an increased hemoglobin content in skin  
48  
49  
516 vessels, EI values are calculated by subtracting LIR values at 510 and 610 nm (mainly  
50  
51  
517 related to melanin absorbance) from the sum of LIR values at 540, 560, and 580 nm, the  
52  
53  
518 absorption peak wavelengths for hemoglobin.  
54  
55  
56  
57

519  
59

60  
61  
62  
63  
64  
65



520 CRO depletion profiles obtained by tape stripping suggested that both ETHO-CRO-X GUM  
1  
521 and ORG-CRO enhanced the penetration of CRO with respect to X GUM. Nonetheless,  
3  
522 the higher CRO amount found in the case of ETHO-CRO-X GUM could be justified the  
4  
6  
523 hypothesis of the formation of a PC depot in the stratum corneum from which CRO can be  
8  
9  
524 released in a controlled fashion (Esposito et al, 2014). Moreover it should be consider the  
10  
11  
525 heterogeneous distribution of CRO in ETHO-CRO-X GUM, indeed a portion of CRO is  
13  
14  
526 distributed in the multilamellar vesicles, while the untrapped portion of CRO is free in the  
15  
16  
527 gel. Due to its heterogeneous distribution, CRO interact with the skin in different ways,  
18  
19  
528 resulting in a sustained presence in the *stratum corneum*.

20  
21  
22  
529 Surprisingly, the profile obtained by reflectance spectroscopy evidenced an initial higher  
24  
25  
530 anti-inflammatory activity exploited by ETHO-CRO-X GUM, followed by a more  
26  
27  
531 pronounced decrease with respect to ORG-CRO. Notably, in the case of ETHO-CRO-X  
29  
30  
532 GUM, after 3 and 6 hs, CRO probably reached the dermal zone, afterwards the drug was  
31  
32  
533 rapidly removed by the blood stream. It could be tentatively supposed that after 1 h from  
34  
35  
534 ETHO-CRO-X GUM removal, CRO could exert an intense anti-inflammatory activity due to  
36  
37  
535 the presence of a high amount of ethanol, acting as penetration enhancer (Harrison et al,  
38  
39  
536 2004). Indeed ethanol is known to penetrate through intercellular lipids, increasing the cell  
41  
42  
537 membrane lipid fluidity and decreasing the density of lipid multilayer (Verma end Pathak,  
43  
44  
538 2010; Toitou and Godin, 2007). However the higher enhancing effect of ETHO cannot be  
46  
47  
539 only due to the presence of ethanol, which is a permeability enhancer, but overall in the  
48  
49  
540 resulting drug carrier system as a whole. As suggested by other authors, it seems  
51  
52  
541 plausible that ETHO-CRO could form a colloidal film on the skin surface, this film would  
53  
54  
542 result in a reduction of skin dehydration and an impairment of the barrier properties  
56  
57  
543 (Bodade et al, 2010). In addition the well known flexibility of ETHO can also be a critical  
58  
59  
544 parameter (Mishra et al, 2013). Anyway both ETHO-CRO-X GUM and ORG-CRO were  
60  
61  
62  
63  
64  
65

545 able to increase CRO penetration. Indeed it is reasonable to suppose a strong interaction  
1  
546 of PC with the *stratum corneum* lipids (El Maghraby and Williams, 2009; Sataphy et al,  
3  
547 2013) resulting in a high concentration of CRO in the vascularized section of the skin,  
4  
6  
548 where it displayed an anti-inflammatory activity.  
8  
9

10  
549

## 530 **5. Conclusions**

14  
15  
551

17  
552 ETHO and ORG have been demonstrated to be efficient vehicles for CRO administration  
19  
20  
553 on skin. Particularly ORG was able to better control CRO labile stability.  
21

22  
554 *In vivo* studies have demonstrated that thanks to the peculiar supramolecular organization  
24  
555 of PC, both ETHO-CRO and ORG-CRO vehicles enhanced CRO absorption through skin,  
26  
556 suggesting their suitability to treat inflammatory skin disorders. Moreover CRO can also  
27  
29  
557 have a protective effect on the surface of the skin, like sunscreens. This double effect  
31  
32  
558 could be useful for instance in melanoma prevention and therapy. Nonetheless, to verify  
34  
559 this hypothesis animal studies should be performed.  
36

37  
560

## 40 41 **Acknowledgements**

42  
562 The authors are grateful to Sarah Villebrun from Institut Galien Paris-Sud, Châtenay-  
44  
45  
563 Malabry, France for rheological characterization.  
47

48  
564

## 50 51 **Ethical approval**

52  
565  
566 All procedures performed in studies involving human participants were in accordance with  
54  
55  
567 the ethical standards of the national research committee and with the 1964 Helsinki  
57  
568 declaration and its later amendments or comparable ethical standards.  
59

60  
569

570 **Informed consent**

1  
2  
3 571 Informed consent was obtained from all individual participants included in the study.

4  
5 572

6  
7  
8  
9  
10  
11  
12  
13  
14  
15  
16  
17  
18  
19  
20  
21  
22  
23  
24  
25  
26  
27  
28  
29  
30  
31  
32  
33  
34  
35  
36  
37  
38  
39  
40  
41  
42  
43  
44  
45  
46  
47  
48  
49  
50  
51  
52  
53  
54  
55  
56  
57  
58  
59  
60  
61  
62  
63  
64  
65

573 **References**

1  
574  
3  
4  
575 S.H. Alavizadeh, H. Hosseinzadeh, Bioactivity assessment and toxicity of crocin: A  
6  
576 comprehensive review. *Food Chem. Toxicol.* 64, 65-80 (2014).  
8  
9  
577  
10  
11  
578 A. Asai, T. Nakano, M. Takahashi, A. Nagao, Orally administered crocetin and crocins are  
13  
579 absorbed into blood plasma as crocetin and its glucuronide conjugates in mice. *J. Agr.*  
15  
580 *Food. Chem.* 53, 7302-7306 (2005).  
18  
19  
581  
20  
21  
22  
582 S.S. Bodade, K.S. Shaikh, M.S. Kamble, P.D. Chaudhari, A study on ethosomes as mode  
24  
583 for transdermal delivery of an antidiabetic drug. *Drug Delivery* 20, 40-46 (2013).  
26  
27  
28  
584  
30  
31  
585 M. Changez, J. Chander, A.K. Dinda, Transdermal permeation of tetracaine hydrochloride  
32  
586 by lecithin microemulsion: in vivo. *Coll. Surf. B Biointerfaces* 48, 58-66 (2006).  
35  
36  
587  
37  
38  
588 E. Christodoulou, N.P. Kadoglou, N. Kostomitsopoulos, G. Valsami, Saffron: A natural  
40  
589 product with potential pharmaceutical applications. *J. Pharm. Pharmacol.* 67, 1634-1649  
42  
590 (2015).  
43  
44  
45  
591  
47  
48  
592 K.S. Chun, J. Kundu, J.K. Kundu, Y.J. Surh, Targeting Nrf2-Keap1 signaling for  
49  
593 chemoprevention of skin carcinogenesis with bioactive phytochemicals. *Toxicol. Lett.* 229,  
52  
594 73-84 (2014).  
54  
55

595

57

58

59

60

61

62

63

64

65

- 596 G.M. El Maghraby, A.C. Williams, Vesicular systems for delivering conventional small  
1  
597 organic molecules and larger macromolecules to and through human skin. *Expert Opin.*  
3  
598 *Drug Deliv.* 6, 149-63 (2009).  
4  
599  
6  
600 J. Escribano, G.L. Alonso, M. Coca-Prados, J.A. Fernandez, Crocin, safranal and  
8  
601 picrocrocin from saffron (*Crocus sativus* L.) inhibit the growth of human cancer cells in  
10  
602 vitro. *Cancer Lett.* 100, 23-30 (1996).  
12  
603  
14  
604 E. Esposito, R. Cortesi, M. Drechsler, L. Paccamiccio, P. Mariani, C. Contado, E. Stellin,  
16  
605 E. Menegatti, F. Bonina, C. Puglia, Cubosome dispersions as delivery systems for  
18  
606 percutaneous administration of indomethacin. *Pharm. Res.* 22, 2163-2173 (2005).  
20  
607  
22  
608 E. Esposito, P. Mariani, L. Ravani, C. Contado, M. Volta, S. Bido, M. Drechsler, S.  
24  
609 Mazzoni, E. Menegatti, M. Morari, R. Cortesi, Nanoparticulate lipid dispersions for  
26  
610 bromocriptine delivery: characterization and in vivo study. *Eur. J. Pharm. Biopharm.* 80,  
28  
611 306-314 (2012).  
30  
612  
32  
613 E. Esposito, E. Menegatti, R. Cortesi, Design and characterization of fenretinide containing  
34  
614 organogels. *Mat. Sci. Eng. C* 33, 383-389 (2013).  
36  
615  
38  
616 E. Esposito, L. Ravani, P. Mariani, N. Huang, P. Boldrini, M. Drechsler, G. Valacchi, R.  
40  
617 Cortesi, C. Puglia, Effect of nanostructured lipid vehicles on percutaneous absorption of  
42  
618 curcumin, *Eur. J. Pharm. Biopharm.* 86, 121-132 (2014).  
44  
619  
46  
620 Z. Fiume, Final report on the safety assessment of lecithin and hydrogenated lecithin. *Int.*  
48  
621 *J. Toxicol.* 20, 21-45 (2001).  
50  
52  
54  
55  
56  
57  
58  
59  
60  
61  
62  
63  
64  
65

622  
1  
623  
3  
624  
4  
5  
6  
625  
8  
626  
9  
10  
627  
11  
12  
13  
628  
14  
15  
629  
16  
17  
18  
630  
19  
20  
631  
21  
22  
23  
632  
24  
25  
633  
26  
27  
28  
634  
29  
30  
635  
31  
32  
33  
636  
34  
35  
637  
36  
37  
38  
638  
39  
40  
639  
41  
42  
640  
43  
44  
45  
641  
46  
47  
642  
48  
49  
50  
643  
51  
52  
644  
53  
54  
55  
645  
56  
57  
646  
58  
59  
647  
60  
61  
62  
63  
64  
65

B. Godin, E. Touitou, Ethosomes: new prospects in transdermal delivery. Crit. Rev. Ther. Drug Carrier Syst. 20, 63-102 (2003).

J. Grdadolnik, J. Kidric, D. Hadzi, Hydration of phosphatidylcholine reverse micelles and multilayers-an infrared spectroscopic study. Chem. Phys. Lipids 59, 57-68 (1991).

G.I. Harrison, A.R. Young, S.B. McMahon, Ultraviolet Radiation-Induced Inflammation as a Model for Cutaneous Hyperalgesia. J. Invest. Dermatol. 122, 183-9 (2004).

K. Hashizaki, N. Tamaki, H. Taguki, Y. Saito, K. Tsuchiya, H. Sakai, M. Abe, Rheological behavior of worm-like micelles in a mixed nonionic surfactant system of a polyoxyethylene phytosterol and a glycerin fatty acid monoester. Chem. Pharm. Bull 56, 1682-1686 (2008).

S. Jain, A.K. Tiwary, B. Sapra, N.K. Jain, Formulation and evaluation of ethosomes for transdermal delivery of lamivudine. AAPS PharmSciTech. 8, 249 E1–E9 (2007).

T. Konoshima, M. Takasaki, H. Tokuda, S. Morimoto, H. Tanaka, E. Kawata, L.J. Xuan, H. Saito, M. Sugiura, J. Molnar, Y. Shoyama, Crocin and crocetin derivatives inhibit skin tumor promotion in mice. Phytother. Res. 12, 400-404 (1998).

R. Kumar, O.P. Katare, Lecithin organogels as a potential phospholipid-structured system for topical drug delivery: A review. AAPS PharmSciTech 6, E298–E310 (2005).

P.L. Luisi, R. Scartazzini, G. Haering, P. Schurtenberger, Organogels from water-in-oil microemulsions. Colloid Polym. Sci. 268, 356-374 (1990).

648  
1  
2  
3  
4  
5  
6  
7  
8  
9  
10  
11  
12  
13  
14  
15  
16  
17  
18  
19  
20  
21  
22  
23  
24  
25  
26  
27  
28  
29  
30  
31  
32  
33  
34  
35  
36  
37  
38  
39  
40  
41  
42  
43  
44  
45  
46  
47  
48  
49  
50  
51  
52  
53  
54  
55  
56  
57  
58  
59  
60  
61  
62  
63  
64  
65

M. Marcotte, R. Taherian Hoshahili, H.S. Ramaswamy, Rheological properties of selected hydrocol as a function of concentration and temperature. Food Res. Intern. 34, 695-703 (2001).

S.M. Meeran, M. Vaid, T. Punathil, S.K. Katiyar, Dietary grape seed proanthocyanidins inhibit 12-Otetradecanoyl phorbol-13-acetate-caused skin tumor promotion in 7,12-dimethylbenz[a]anthracene-initiated mouse skin, which is associated with the inhibition of inflammatory responses. Carcinogenesis 30, 520-528 (2009).

A.D. Mishra, C.N. Patel, D.R. Shah, Formulation and optimization of ethosomes for transdermal delivery of ropinirole hydrochloride. Curr. Drug Deliv. 10, 500-516 (2013).

A. Mittal, C.A. Elmets, S.K. Katiyar, Dietary feeding of proanthocyanidins from grape seeds prevents photocarcinogenesis in SKH-1 hairless mice: relationship to decreased fat and lipid peroxidation. Carcinogenesis 24,1379-1388 (2003).

K.N. Nam, Y.M. Park, H.J. Jung, J.Y. Lee, B. Min, S. Park, W. Jung, K. Cho, J. Park, I. Kang, J.Hong, E.H. Lee, Anti-inflammatory effects of crocin and crocetin in rat brain microglial cells. Eur. J. Pharmacol. 648, 110-6 (2010).

V. Nandakumar, T. Singh, S.K. Katiyar, Multi-targeted prevention and therapy of cancer by proanthocyanidins. Cancer Letters 269, 378-387 (2008).

671  
1  
672  
3  
673  
4  
6  
674  
8  
675  
10  
676  
11  
677  
13  
678  
15  
679  
16  
680  
18  
681  
20  
682  
21  
683  
22  
684  
23  
685  
25  
686  
26  
687  
27  
688  
28  
689  
30  
690  
31  
691  
32  
692  
33  
693  
35  
694  
36  
695  
37  
696  
38  
697  
39  
698  
40  
699  
41  
700  
42  
701  
43  
702  
44  
703  
45  
704  
46  
705  
47  
706  
48  
707  
49  
708  
50  
709  
51  
710  
52  
711  
53  
712  
54  
713  
55  
714  
56  
715  
57  
716  
58  
717  
59  
718  
60  
719  
61  
720  
62  
721  
63  
722  
64  
723  
65

K.D. Patil, S.R. Bakliwal, S.P. Pawar, Organogel: topical and transdermal drug delivery system. *Int. J Pharm. Res. Dev.* 3, 58-66 (2011).

R. Pecora, Dynamic light scattering measurement of nanometer particles in liquids. *J. Nanoparticle Res.* 2, 123-131 (2000).

W.J. Pugh, Kinetics of product stability. In: Aulton ME (Ed). *Aultons's Pharmaceutics. The design and manufacture of the medicines.* 3rd ed. London: Churchill Livingstone Elsevier p:99-107 (2007).

S. Raut, S.S. Bhadoriya, V. Uplanchiwar, V. Mishra, A. Gahane, S.K. Jain, Lecithin organogel: A unique micellar system for the delivery of bioactive agents in the treatment of skin aging. *Acta Pharm. Sin. B* 2, 8-15 (2012).

F.M. Robertson. Skin carcinogenesis. In Schwab M, editor. *Encyclopedia of cancer* Springer Berlin Heidelberg. p 3432-3435 (2012).

D. Satapathy, D. Biswas, B. Behera, S.S. Sagiri, K. Pal, K. Pramanik, Sunflower-oil-based lecithin organogels as matrices for controlled drug delivery. *J. Appl. Polym. Sci.* 129, 585-594 (2013).

Y.A. Schipunov, A micellar system with unique properties, *Colloids Surf. A* 185:541-554 (2001).



696 Y.A. Schipunov, H. Hoffmann. Thinning and thickening effects induced by shearing in  
1  
697 lecithin solutions of polymer-like micelles. *Rheol. Acta* 39, 542-553 (2000).  
3  
698  
4  
699 K.-W. Song, Y.-S. Kim, G.S. Chang, Rheology of concentrated xanthan gum solutions:  
6  
700 Steady shear flow behaviour. *Fiber Polym.* 7, 129-138 (2006).  
8  
10  
11  
701  
13  
702 Y.J. Surh, Cancer chemoprevention with dietary phytochemicals. *Nat. Rev. Cancer* 10,  
15  
703 768-80 (2003).  
16  
18  
704  
20  
705 W. Tian, Q. Hu, Y. Xu, Effect of soybean-lecithin as an enhancer of buccal mucosa  
21  
22  
23  
706 absorption of insulin. *Biomed. Mater Eng.* 22, 171-178 (2012).  
25  
26  
707  
28  
29  
708 E. Touitou, N. Dayan, L. Bergelson, B. Godin, M. Eliaz, Ethosomes-novel vesicular carriers  
31  
709 for enhanced delivery: characterization and skin penetration properties. *J. Control.*  
32  
33  
34  
710 *Release* 65, 403-18 (2000).  
36  
711  
38  
39  
712 E. Touitou, B. Godin, Dermal drug delivery with ethosomes: therapeutic potential. *Therapy*  
41  
713 4, 465-472 (2007).  
43  
44  
714  
46  
715 M. Tsimidou, E. Tsatsaroni, Stability of saffron pigments in aqueous extracts. *J. Food Sci.*  
48  
716 58, 1073-1075 (1993).  
49  
50  
51  
717  
53  
718 P. Verma, K. Pathak, Therapeutic and cosmeceutical potential of ethosomes: An overview.  
55  
56  
719 *J. Adv. Pharm. Technol. Res.* 1, 274-282 (2010).  
58  
720  
60  
61  
62  
63  
64  
65

721 A. Vintiloiu, J.-C. Leroux, Organogels and their use in drug delivery: a review. J Control  
1  
722 Release 125, 179-192 (2008).  
3  
723  
4  
6  
724 H. Wanga, T.O. Khorb, L. Shu, Z. Su, F. Fuentes, J.-H. Lee, A.-N.T. Kong, Plants against  
8  
725 cancer: a review on natural phytochemicals in preventing and treating cancers and their  
10  
726 druggability. Anti-cancer Agents Med. Chem. 12,1281-1305 (2012).  
11  
13  
727  
15  
16  
728 C.-J. Weng, G.-C. Yen, Chemopreventive effects of dietary phytochemicals against cancer  
18  
729 invasion and metastasis: Phenolic acids, monophenol, polyphenol and their derivatives.  
20  
730 Cancer Treat. Rev. 38, 76-87 (2012).  
21  
22  
23  
731  
25  
732 P. Winterhalter, R.M. Straubinger, Saffron, renewed interest in an ancient spice. Food  
27  
733 Rev. Int. 16, 39-59 (2000).  
28  
30  
734  
31  
32  
33  
735 J. Wohlrab, T. Klapperstück, H.W. Reinhardt, M. Albrecht, Interaction of epicutaneously  
35  
736 applied lipids with stratum corneum depends on the presence of either emulsifiers or  
37  
737 hydrogenated phosphatidylcholine. Skin Pharmacol. Physiol. 23, 298-305 (2010).  
38  
40

738  
42  
43  
44  
45  
46  
47  
48  
49  
50  
51  
52  
53  
54  
55  
56  
57  
58  
59  
60  
61  
62  
63  
64  
65

739 **FIGURE LEGENDS**

1

2

740

4

741

7

742

9

10

743

12

744

13

745

17

746

19

747

22

748

24

749

25

750

29

751

31

752

34

753

36

37

754

39

40

755

42

756

43

757

47

758

48

759

50

760

52

761

54

55

56

57

58

59

60

61

62

63

64

65

**Figure 1.** Cryo-transmission electron microscopy images (cryo-TEM) of ETHO (A, B) and ETHO-CRO (C, D). Bar corresponds to 200 or 85 nm in panels A, C and B, D respectively.

**Figure 2.** Photographs and schematic drawings of ETHO-CRO (A) and ORG-CRO (B). In particular in panel A is drawn the possible distribution of CRO (●) in the aqueous environment inside and outside ETHO-CRO vesicles, while in the case of ORG-CRO (B) CRO is mainly located in the aqueous domain inside the reverse micelles.

**Figure 3.** Variation of CRO residual content in ETHO-CRO (grey), ORG-CRO (light grey) and CRO aqueous solution (black) as a function of time. The formulations were stored in glass containers at 25°C for 3 months. Data are the means of 5 analyses on different batches of the same type of formulations. Standard deviations were comprised between ± 5%.

**Figure 4.** Rheological flow curves for ETHO-CRO-X GUM (A), ORG-CRO (B) and X GUM (C), determined at 25 (grey line) and 35°C (black line). The geometry used was an aluminium cone-plate. Flow curves were obtained by increasing the shear rate from 0.01 s<sup>-1</sup> to 5000 s<sup>-1</sup> with 5 points per decade, each point was maintained for a duration of 180 s in order to perform measurements in the permanent regime. Data are the means of 3 analyses on different batches of the same type of formulations.

762 **Figure 5.** Tape stripping evaluation. (A) Scheme of the forearm of the volunteers depicting  
1  
763 the modality of application of the formulations. (B) CRO amount in the *stratum corneum*  
3  
764 after ETHO-CRO-X GUM, ORG-CRO and X GUM-CRO application, removal and tape  
4  
6  
765 stripping. Tape stripping was performed after 1 (□), 3 (■), and 6 (■) hours from the  
8  
766 removal of formulations (B). Details are reported in the experimental section. Data  
9  
10  
11  
767 represent the mean for ten subjects.  
13

768  
15  
16  
769 **Figure 6.** Anti-inflammatory effect evaluation. (A) Scheme of the forearm of the volunteers  
18  
770 depicting the modality of application of the formulations. (B) Variation of percentage of  
20  
21  
771 erythema index (P.I.E) after topical application and removal of ETHO-CRO-X GUM and  
23  
772 ORG-CRO. P.I.E. evaluation was performed after 1 (□), 3 (■), and 6 (■) hours from  
25  
773 the removal of formulations. Details are reported in the experimental section. Data  
26  
27  
28  
774 represent the mean for ten subjects.  
30

775

32  
33  
34  
35  
36  
37  
38  
39  
40  
41  
42  
43  
44  
45  
46  
47  
48  
49  
50  
51  
52  
53  
54  
55  
56  
57  
58  
59  
60  
61  
62  
63  
64  
65

776 Table 1: Composition of formulations employed in this study  
 777

<i>Formulations</i>	<i>Soy phosphatidylcholine % w/w</i>	<i>Ethanol % w/w</i>	<i>Isopropyl palmitate % w/w</i>	<i>Crocin % w/w</i>	<i>Aqueous phase* % w/w</i>
ETHO	3.0	27.0	-	-	70.00 (IPB)*
ETHO-CRO	3.0	27.0	-	0.05	69.50 (IPB)*
ORG	14.7	-	85.12	-	0.18 (water)
ORG-CRO	14.7	-	85.12	0.05	0.13 (water)

\* isotonic Palitzsch buffer

780 Table 2: Dimensional parameters of ethosomes as determined by PCS.

781

2

3

4

5

6

7

8

9

10

11

12

13

14

15

16

17

18

19

20

21

22

23

24

25

26

27

28

29

30

31

32

33

34

35

36

37

38

39

40

41

42

43

44

45

46

47

48

49

50

51

52

53

54

55

56

57

58

59

60

61

62

63

64

65

<i>Formulations</i>	<i>Z average Size (nm)</i>	<i>Polydispersity index</i>	<i>Typical Intensity distribution</i>		
			<i>peak</i>	<i>nm</i>	<i>area %</i>
ETHO	332.1±20	0.32±0.03	1	440	26
	(492.2±40)*	(0.29±0.08)*	2	162	74
ETHO-CRO	454.0±32	0.38±0.05	1	850	7
	(534.0±50)*	(0.37±0.15)*	2	253	93

\* after 6 months from production

784 Table 3: Entrapment capacity and shelf life values of ethosomes and organogels  
 785

<i>Formulations</i>	<i>EC<sup>a</sup> %</i>	<i>m<sup>b</sup></i>	<i>K<sup>c</sup></i>	<i>t<sub>90</sub>(days)<sup>c</sup></i>	<i>t<sub>1/2</sub>(days)<sup>c</sup></i>
CRO solution	n.d.	0.133	0.306	0.34	2.26
ETHO-CRO	74.44±3.5	0.0063	0.014	7.13	47.14
ORG-CRO	99.5±0.5	0.0012	0.002	37.75	236.51

786 <sup>a</sup>EC: entrapment capacity;

787 <sup>b</sup>slope of the line of log(CRO residual content %) kinetic, calculated as the mean of 3 independent  
 788 determinations, s.d. ≤ 5%

789 <sup>c</sup>K, t<sub>90</sub> and t<sub>1/2</sub> were calculated following eqs. 2, 3 and 4 respectively  
 790

790

21

22

23

24

25

26

27

28

29

30

31

32

33

34

35

36

37

38

39

40

41

42

43

44

45

46

47

48

49

50

51

52

53

54

55

56

57

58

59

60

61

62

63

64

65

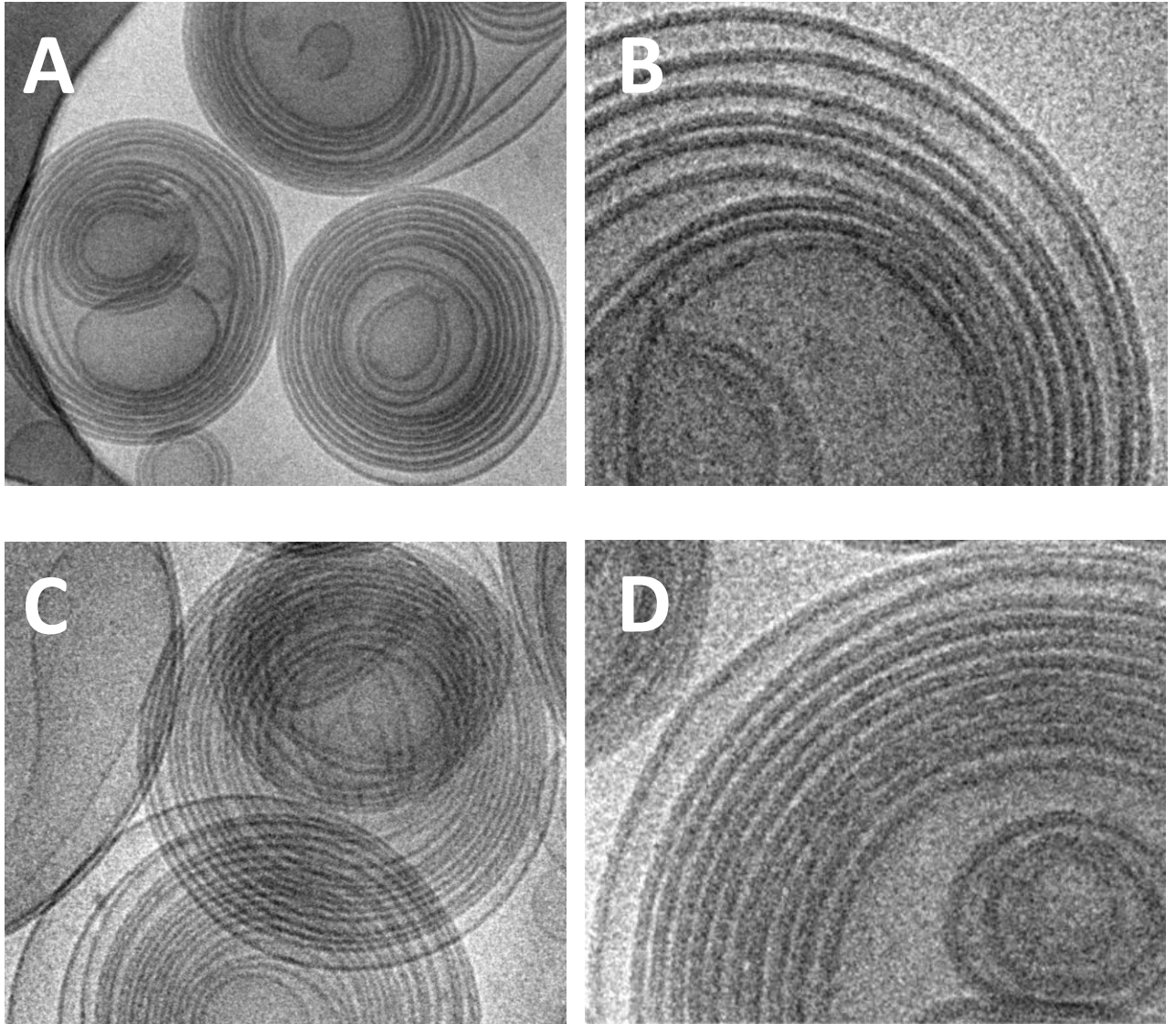
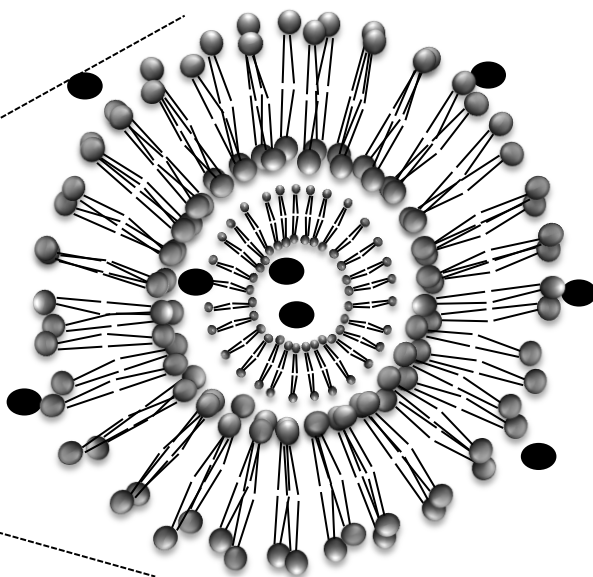
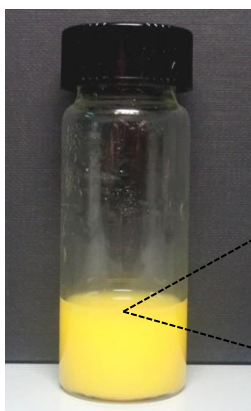


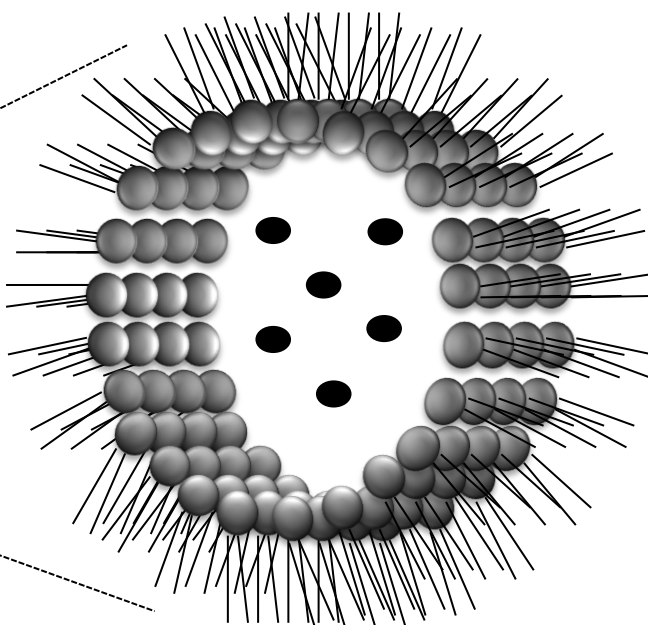
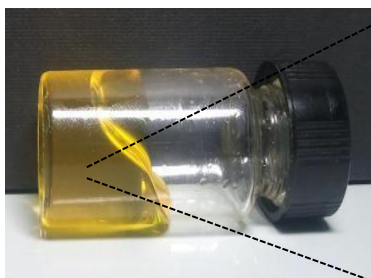
Figure 1



**A**



**B**



● crocin

Figure 2

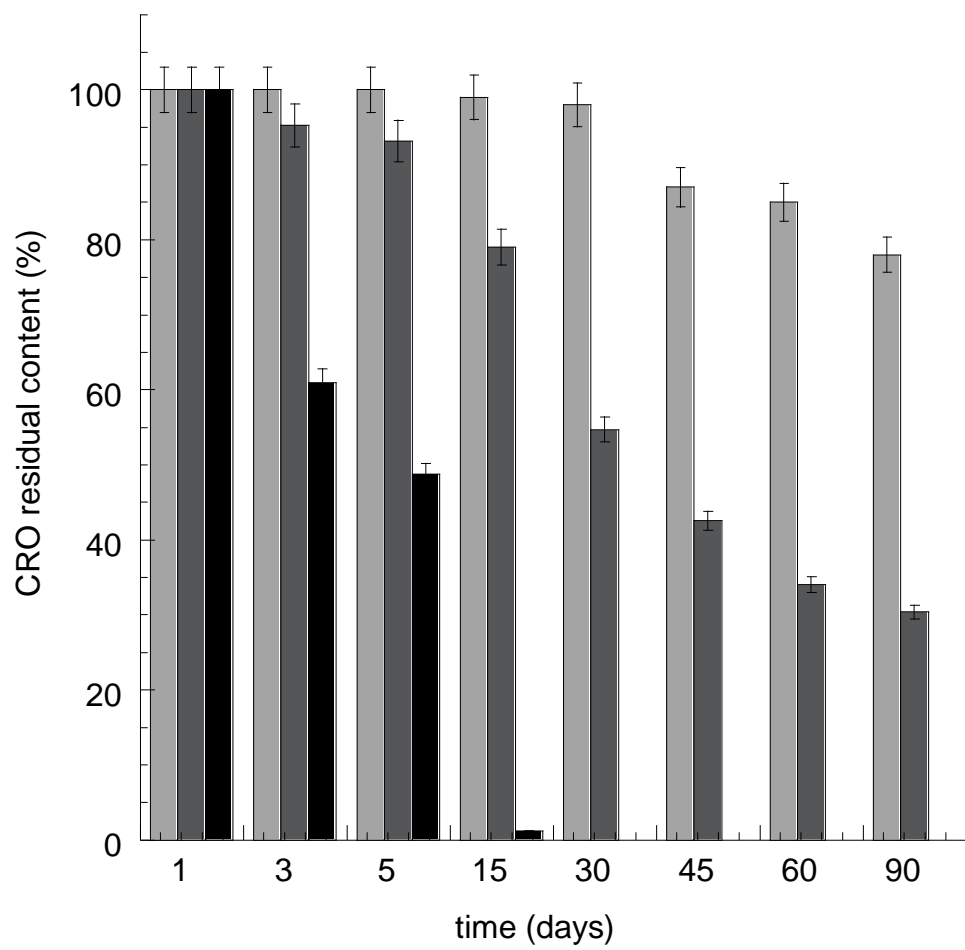


Figure 3

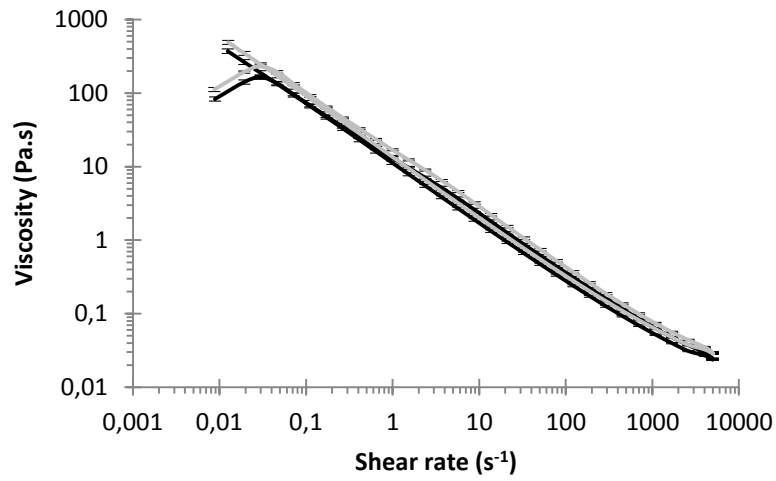
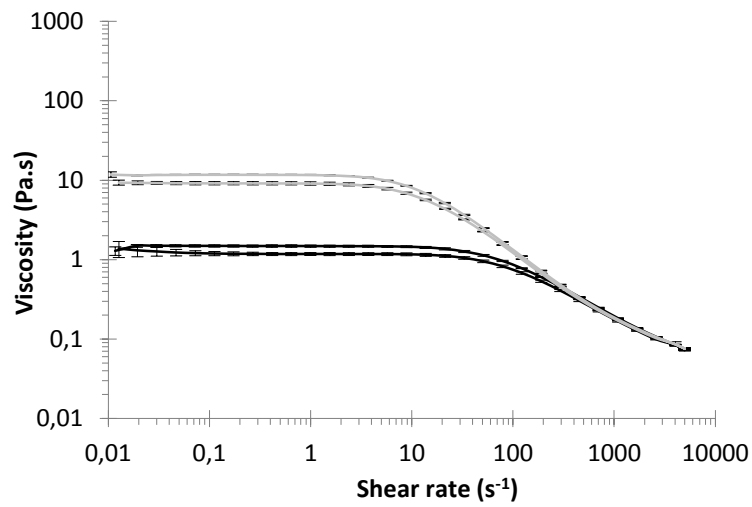
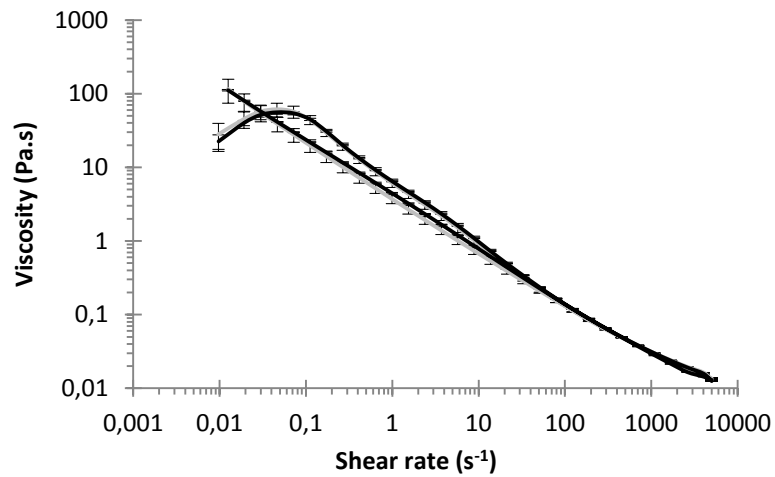
**A****B****C**

Figure 4

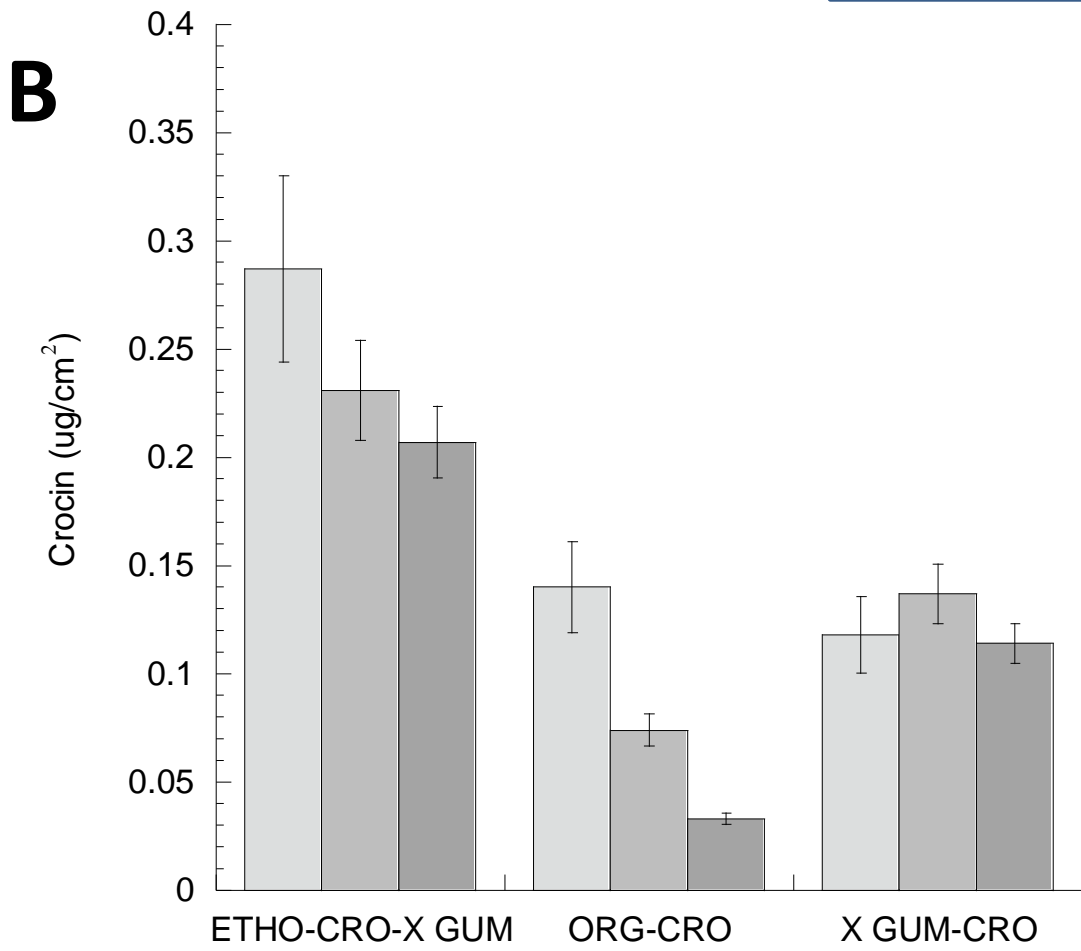
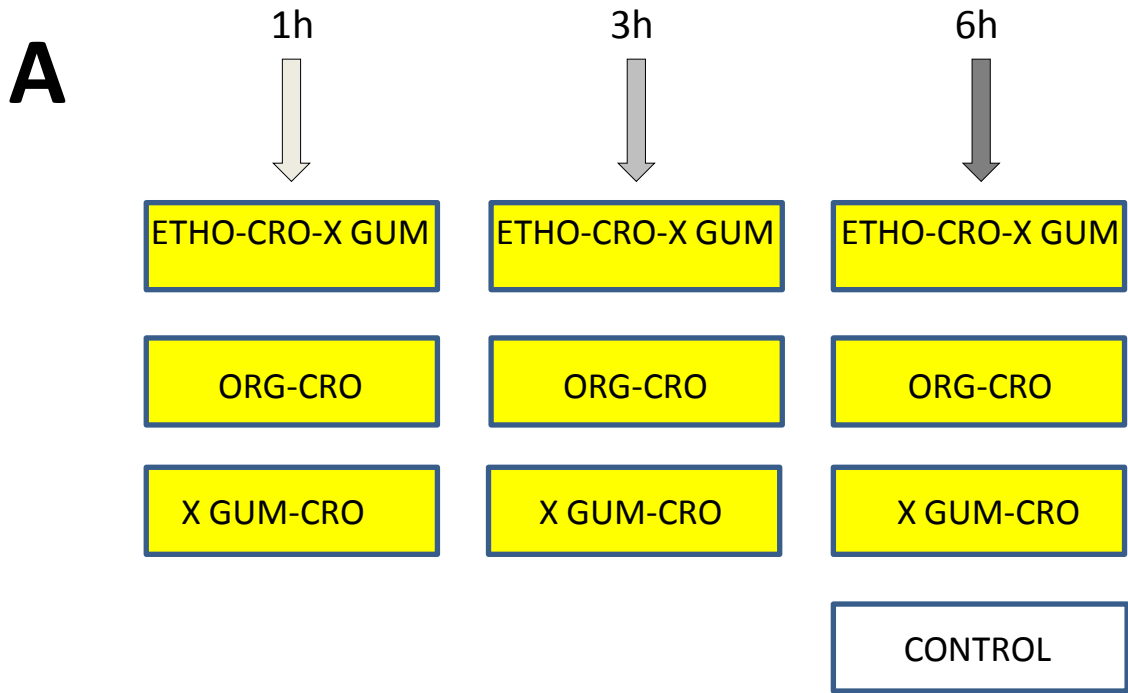


Figure 5

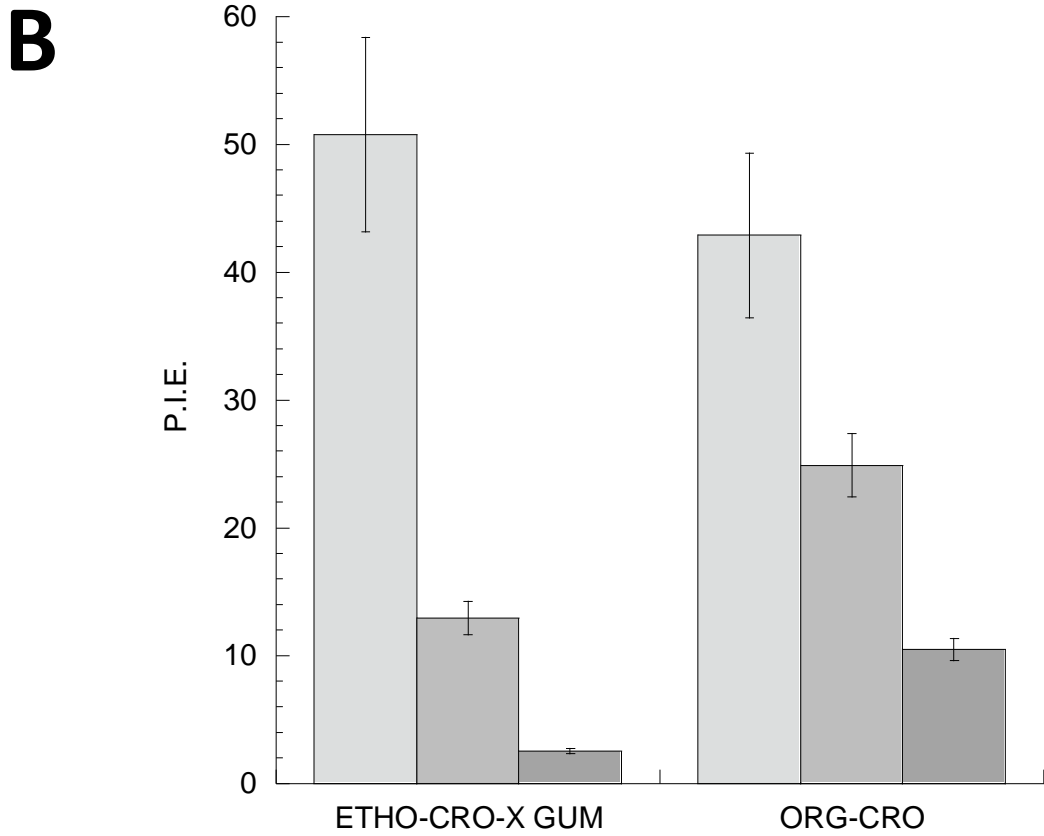
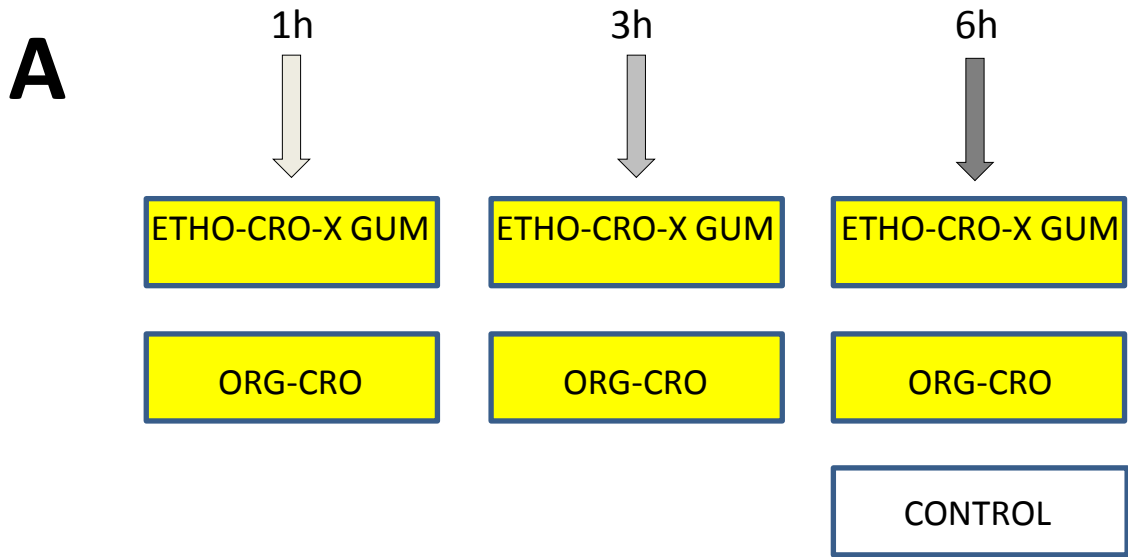


Figure 6

Table 1: Composition of formulations employed in this study

<b>Formulations</b>	<b>Soy phosphatidylcholine % w/w</b>	<b>Ethanol % w/w</b>	<b>Isopropyl palmitate % w/w</b>	<b>Crocin % w/w</b>	<b>Aqueous phase* % w/w</b>
ETHO	3.0	27.0	-	-	70.00 (IPB)
ETHO-CRO	3.0	27.0	-	0.05	69.50 (IPB)
ORG	14.7	-	85.12	-	0.18 (water)
ORG-CRO	14.7	-	85.12	0.05	0.13 (water)

ETHO: ethosome; ETHO-CRO: ethosome prepared in the presence of crocin; ORG: organogel; ORG-CRO: organogel prepared in the presence of crocin; IPB: isotonic Palitzsch buffer

Table 2: Dimensional parameters of ethosomes as determined by PCS.

<i>Formulations</i>	<i>Z average Size (nm)</i>	<i>Polydispersity index</i>	<i>Typical Intensity distribution</i>		
			<i>peak</i>	<i>nm</i>	<i>area %</i>
ETHO	332.1±20	0.32±0.03	1	440	26
	(492.2±40)*	(0.29±0.08)*	2	162	74
ETHO-CRO	454.0±32	0.38±0.05	1	850	7
	(534.0±50)*	(0.37±0.15)*	2	253	93

\* after 6 months from production ETHO: ethosome; ETHO-CRO: ethosome prepared in the presence of crocin

Table 3: Entrapment capacity and shelf life values of ethosomes and organogels

<i>Formulations</i>	<i>EC<sup>a</sup> %</i>	<i>m<sup>b</sup></i>	<i>K<sup>c</sup></i>	<i>t<sub>90</sub>(days)<sup>c</sup></i>	<i>t<sub>1/2</sub>(days)<sup>c</sup></i>
CRO solution	n.d.	0.133	0.306	0.34	2.26
ETHO-CRO	74.44±3.5	0.0063	0.014	7.13	47.14
ORG-CRO	99.5±0.5	0.0012	0.002	37.75	236.51

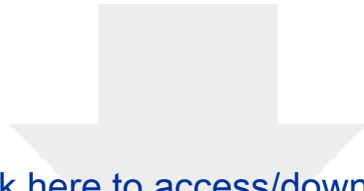
<sup>a</sup>EC: entrapment capacity;

<sup>b</sup>slope of the line of log(CRO residual content %) kinetic, calculated as the mean of 3 independent determinations, s.d. ≤ 5%

<sup>c</sup>K, t<sub>90</sub> and t<sub>1/2</sub> were calculated following eqs. 2, 3 and 4 respectively

CRO solution: aqueous solution of crocin; ETHO-CRO: ethosome prepared in the presence of crocin; ORG-CRO: organogel prepared in the presence of crocin

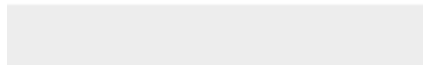


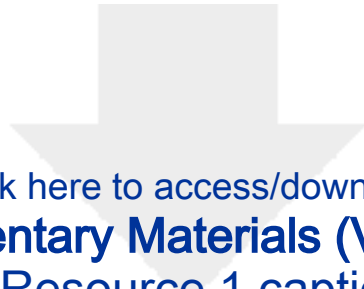


Click here to access/download

**Supplementary Materials (Video Clip)**

Online Resource 1.tif





Click here to access/download

**Supplementary Materials (Video Clip)**  
Online Resource 1 caption.docx

